ISSN 1674-1056
http://cpb.iphy.ac.cn
http://iopscience.iop.org/cpb
中国物理 B
Chinese Physics
中国物理
Chinese Physics B

Influence analysis of symmetry on capsule in six-cylinder-port hohlraum

You Zou(邹游), Wudi Zheng(郑无敌), Xin Li(李欣)

Citation: Chin. Phys. B . 2019, 28(3): 035203. **doi:** 10.1088/1674-1056/28/3/035203
Journal homepage: http://cpb.iphy.ac.cn; http://iopscience.iop.org/cpb

What follows is a list of articles you may be interested in

Rayleigh-Taylor instability at spherical interfaces of incompressible fluids

Hong-Yu Guo(郭宏宇), Li-Feng Wang(王立锋), Wen-Hua Ye(叶文华), Jun-Feng Wu(吴俊峰), Ying-Jun Li(李英骏), Wei-Yan Zhang(张维岩)

Chin. Phys. B . 2018, 27(2): 025206. **doi:** 10.1088/1674-1056/27/2/025206

A new ignition hohlraum design for indirect-drive inertial confinement fusion

Xin Li(李欣), Chang-Shu Wu(吴畅书), Zhen-Sheng Dai(戴振生), Wu-Di Zheng(郑无敌), Jian-Fa Gu(谷建法), Pei-Jun Gu(古培俊), Shi-Yang Zou(邹士阳), Jie Liu(刘杰), Shao-Ping Zhu(朱少平)

Chin. Phys. B . 2016, 25(8): 085202. **doi:** 10.1088/1674-1056/25/8/085202

Effect of inner-surface roughness of conical target on laser absorption and fast electron generation

Wang Huan, Cao Li-Hua, Zhao Zong-Qing, Yu Ming-Yang, Gu Yu-Qiu, He Xian-Tu

Chin. Phys. B . 2014, 23(5): 055202. **doi:** 10.1088/1674-1056/23/5/055202

Diagnostic technique for measuring fusion reaction rate for inertial confinement fusion experiments at Shen Guang-III prototype laser facility

Wang Feng, Peng Xiao-Shi, Kang Dong-Guo, Liu Shen-Ye, Xu Tao

Chin. Phys. B . 2013, 22(11): 115204. **doi:** 10.1088/1674-1056/22/11/115204

Directly driven Rayleigh–Taylor instability of modulated CH targets

Jia Guo, Xiong Jun, Dong Jia-Qin, Xie Zhi-Yong, Wu Jiang

Chin. Phys. B . 2012, 21(9): 095202. **doi:** 10.1088/1674-1056/21/9/095202

Influence analysis of symmetry on capsule in six-cylinder-port hohlraum*

You Zou(邹游)[1,2], Wudi Zheng(郑无敌)[2,†], and Xin Li(李欣)[2]

[1] School of Science, Chongqing University of Technology, Chongqing 400054, China
[2] Institute of Applied Physics and Computational Mathematics, Beijing 100094, China

(Received 30 November 2018; revised manuscript received 14 January 2019; published online 22 February 2019)

We have investigated the flux symmetry on the capsule in a six-cylinder-port hohlraum for improving the design of the hohlraum. The influence factors of drive symmetry on the capsule in the hohlraum are studied, including laser power, laser beams arrangement, hohlraum geometric parameters, plasma condition, capsule convergence, etc. The x-ray radiation flux distribution on the capsule is obtained based on the three-dimensional view factor model. In the six-cylinder-port hohlraum, the main drive asymmetry is the C_{40} mode asymmetry. When the C_{40} mode asymmetry approaches zero, the drive symmetry on the capsule is optimal. Our results demonstrate that in order to have a high flux symmetry on the capsule in the laser main-pulse stage, more negative initial C_{40} modes are needed, which can be realized by adjusting the hohlraum geometry parameters. The hohlraum with column length $L_{\rm H} = 4.81$ mm has an optimal symmetry in the laser main-pulse stage.

Keywords: inertial confinement fusion (ICF), six-cylinder-port hohlraum, flux symmetry, three-dimensional view factor model

PACS: 52.57.–z, 52.57.Bc, 52.38.Dx **DOI:** 10.1088/1674-1056/28/3/035203

1. Introduction

Cylindrical hohlraum is most commonly used in indirect-drive central ignition inertial confinement fusion (ICF).[1] The US National Ignition Facility (NIF) used cylindrical hohlraum with two laser entrance holes (LEHs), but the National Ignition Campaign (NIC) failed because of excessive instability of the capsule implosion and some issues with the hohlraum, such as difficulty in optimizing symmetry and laser plasma interaction (LPI) problem.[2] For optimizing symmetry, spherical hohlraum with 6 LEHs has been proposed.[3–5] However, in spherical hohlraum, the laser spots are very close to LEHs, and therefore, the expanding plasma from plasma bubbles could impede laser beams from entering the hohlraum. To avoid this, six-cylinder-port hohlraum has been proposed.[6,7] Although hohlraums with 6 LEHs lose a considerable amount of radiation energy because of the large number of LEHs, the six-cylinder-port hohlraum combines the advantages of cylindrical geometry and laser beams arrangement with 6 LEHs. In the six-cylinder-port hohlraum, every cylinder is relatively independent, and the aforementioned issues in the spherical hohlraum are improved.

The capsule flux symmetry is one of the important aspects of indirect-drive ICF.[8–13] Typical capsule convergence ratios range from 25 to 45, so that the initial drive asymmetry no more than 1% is required. In cylindrical hohlraums, the Legendre polynomial modes P_2 and P_4 of the flux on the capsule are the main asymmetry modes required to be controlled. The asymmetry is controlled using three or four spot rings. The adjustment of the power ratio between the rings can reduce the P_2 asymmetry. The P_4 asymmetry is controlled by choosing suitable positions for the laser spots.[14–18] The six-cylinder-port hohlraum with octahedral symmetry[11] has advantages over cylindrical hohlraum with 2 LEHs. Because of the symmetrical geometry with 6 LEHs, there is no P_l $(l < 4)$ asymmetry mode.[11] Higher modes with $l > 4$ can be neglected because they quickly smoothen themselves with a suitable choice of hohlraum size (these high modes are below the order of 10^{-4}); so, only the P_4 asymmetry mode needs to be controlled. In six-cylinder-port hohlraum, through adjusting the incident angle of laser beams, the effects of laser spots and LEHs are compensated, and the P_4 asymmetry mode is close to zero.[6]

The sources of asymmetry on the capsule are laser spots and LEHs. Changes in geometrical parameter and evolutions of various physical processes can be attributed to the variations of laser spots and LEHs. The relative intensity, position, and size of laser spots influence their contribution. The laser power and albedo of hohlraum wall affect the relative intensity of laser spots, and the incident angle of laser beams influences their position and size. The shrinking of LEHs and the movement of hohlraum wall[19] caused by plasma expansion affect the symmetry too. In this study, based on the three-dimensional (3D) view factor model,[20] the factors that influence the symmetry on the capsule have been investigated for improving the design of the six-cylinder-port hohlraum. The

*Project supported by the National Natural Science Foundation of China (Grant No. 11705010) and China Postdoctoral Science Foundation (Grant No. 2017M610821).

†Corresponding author. E-mail: zheng_wudi@iapcm.ac.cn

© 2019 Chinese Physical Society and IOP Publishing Ltd

effect of capsule compression on symmetry has also been studied. The variation in flux symmetry with changes in various geometric parameters has been simulated. Based on these simulation results, the design of the six-cylinder-port hohlraum has been optimized.

This paper is arranged as follows. In Section 2, the characteristic quantities for describing the flux symmetry on the capsule are introduced. In Section 3, based on the 3D view factor model, the simulation results of various factors influencing the flux symmetry on the capsule are discussed. In Section 4, a new design for the six-cylinder-port hohlraum is proposed. In Section 5, the conclusions based on the results obtained in the study are presented.

2. Characteristic quantities

There are, in general, two measurements of the radiation flux symmetry on the capsule; one is peak-to-valley $\varepsilon_{\rm ptv}$ expressed as Eq. (1) and the other is root-mean-square $\varepsilon_{\rm rms}$ expressed as Eq. (2).[21]

$$\varepsilon_{\rm ptv} = \frac{1}{2}\left(S_{\max}-S_{\min}\right)/S_0, \tag{1}$$

$$\begin{aligned}\varepsilon_{\rm rms} &= \left\{\frac{1}{4\pi}\int\left[S_{\rm c}(\boldsymbol{r})/S_0-1\right]^2{\rm d}\Omega\right\}^{1/2}\\ &= \left\{\frac{1}{4\pi R_{\rm c}^2}\int\left[S_{\rm c}(\boldsymbol{r})/S_0-1\right]^2{\rm d}A\right\}^{1/2}\\ &= \left\{\frac{1}{4\pi R_{\rm c}^2}\sum\left[S_{\rm c}(\boldsymbol{r}_i)/S_0-1\right]^2{\rm d}A_i\right\}^{1/2}.\end{aligned} \tag{2}$$

Here, $S_{\rm c}$ is the radiation flux distribution on the capsule, $R_{\rm c}$ is the radius of the capsule, and ${\rm d}A_i$ is the area of element i on the capsule. $S_{\max}$ and $S_{\min}$ are the maximum and minimum radiation flux intensities on the capsule, respectively. S_0 is the average radiation flux intensity on the capsule, which is given by

$$S_0 = \frac{1}{4\pi R_{\rm c}^2}\int S_{\rm c}(\boldsymbol{r})\,{\rm d}A = \frac{1}{4\pi R_{\rm c}^2}\sum S_{\rm c}(\boldsymbol{r}_i)\,{\rm d}A_i. \tag{3}$$

The radiation flux on the capsule has a significant influence on the compression of the capsule. Because different modes have different response on the behavior of capsule implosion, it is necessary to know the amplitude of various modes. The radiation flux distribution on the capsule can be represented by a spherical harmonic function

$$S_{\rm c}(\Omega)/S_0 = \sum_{lm} C_{lm}Y_{lm}(\Omega). \tag{4}$$

$Y_{lm}(\Omega)$ is an l, m degree spherical harmonic. C_{lm} is a spherical harmonic coefficient given by

$$C_{lm} = \sqrt{\frac{1}{4\pi}}\int Y_{lm}^{*}(\Omega)\frac{S_{\rm c}(\Omega)}{S_0}{\rm d}\Omega. \tag{5}$$

The correlation between the spherical harmonic coefficients and $\varepsilon_{\rm rms}$ can be expressed using Eq. (6)

$$\varepsilon_{\rm rms} = \left(\sum_{l=1}^{\infty}\sum_{m=-l}^{+l}|C_{lm}|^2\right)^{1/2}. \tag{6}$$

$\varepsilon_{\rm ptv}$ cannot describe the flux asymmetry globally; so, in this study, we are more focused on $\varepsilon_{\rm rms}$ and C_{lm}, especially C_{40}.

3. Simulation results

In order to realize the sensitivity of various influence factors on capsule drive asymmetry, the single factor effect is studied. In our simulations, unless otherwise stated, the geometric parameters of the hohlraum are shown in Figs. 1(a) and 1(b). The relative intensity of spot changes with the temperature in the hohlraum. The relative fluxes of the laser spot, the hohlraum wall, and the LEH are simply approximated as 2, 1, and 0, respectively. The nominal spot is 400 μm×600 μm at the best focus.

There are two sources of asymmetry on the capsule: the laser spots yield positive contribution, and the LEHs generate negative contribution. In the six-cylinder-port hohlraum with geometric parameters as shown in Fig. 1,[6] the contribution of laser spots is $C_{40}=0.19\%$, $\varepsilon_{\rm rms}=0.29\%$, and the contribution of LEHs is $C_{40}=-0.34\%$, $\varepsilon_{\rm rms}=0.46\%$. The total asymmetry on the capsule is the superposition of the two contributions: $C_{40}=-0.15\%$, $\varepsilon_{\rm rms}=0.17\%$. The contribution of LEHs is greater; so, the holistic asymmetry on the capsule is negative.

Laser spot is one of the sources of asymmetry on the capsule, and the relative intensity, position, and size of the spot affect its contribution. In a hohlraum, the albedo of hohlraum wall and the laser power can change the relative intensity of laser spots. In the pre-pulse stage, the albedo of hohlraum wall is small, and the relative intensity of spots is high. With the increase of temperature in the hohlraum, the relative intensity between the spot area and the non-spot area gradually decreases. We find that the radiation symmetry on the capsule is optimal while relative intensity of spots keeps the value of 2.3 for the design described above (as shown in Fig. 2(a)). In the main-pulse stage, the intensity ratio of the spot area and the non-spot area is close to 2.0, and the symmetry on the capsule is also good.

In the hohlraum with fixed geometric parameters, laser beam focus size, and laser beam arrangement, the position and shape of the spot are only influenced by the incident angle of the laser (denoted as $\theta_{\rm L}$). In the six-cylinder-port hohlraum, while $\theta_{\rm L}=55^\circ$, the contribution of laser spots to the capsule compensates the negative contribution of LEHs very well; thus, the symmetry on the capsule is the best, but there is still a little C_{40} (Fig. 2(b)). In Fig. 2(b), $\Delta\theta$ is the distance of deviation from the spot position of $\theta_{\rm L}=55^\circ$. With larger $\Delta\theta$, the symmetry is worse.

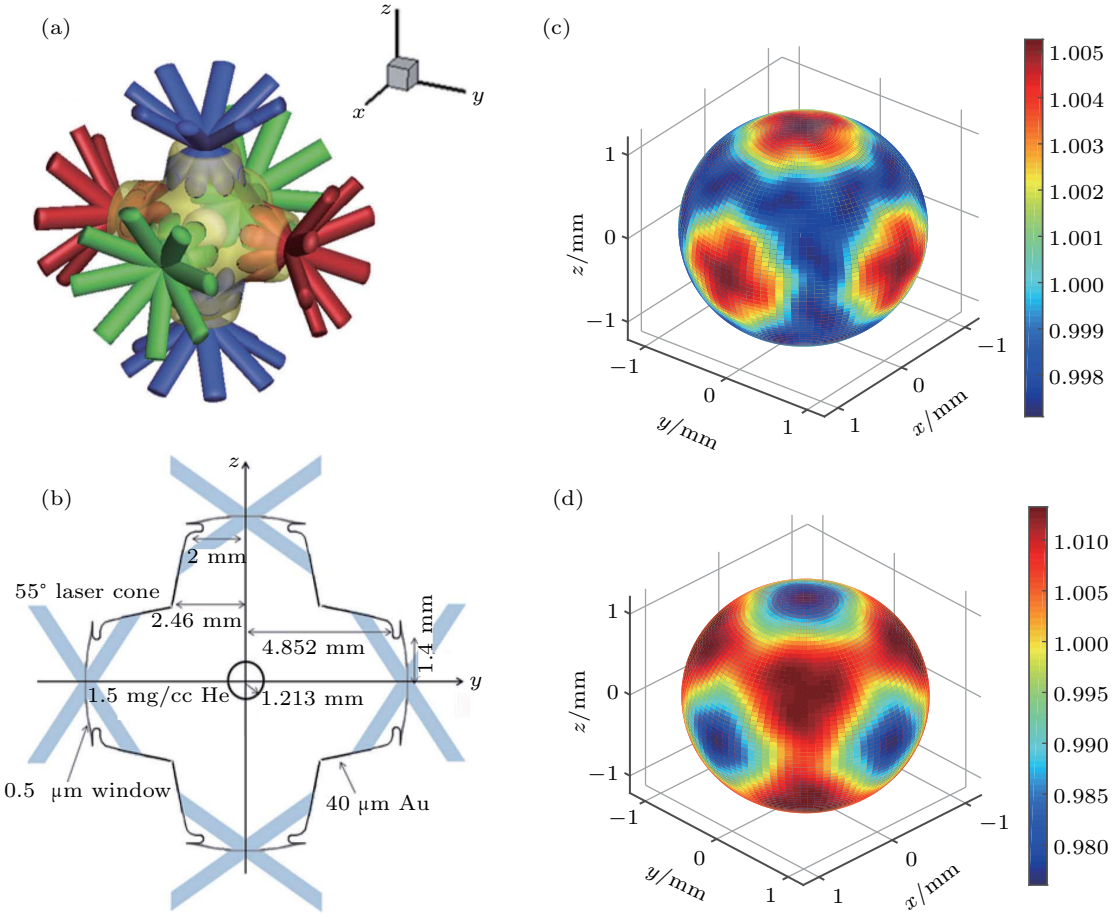


Fig. 1. Schematic diagram of six-cylinder-port hohlraum and two sources of asymmetry. (a) Illustration of the hohlraum with six cylinder ports, 48 laser quads, and centrally located fusion capsule. (b) Hohlraum geometry. (c) and (d) Radiation flux distributions on the capsule only with laser spots and LEHs, respectively.

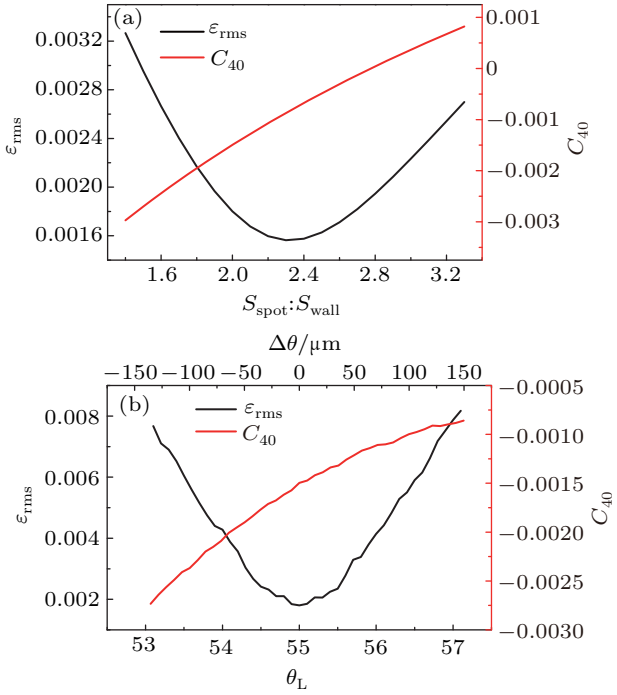


Fig. 2. (a) Flux symmetry as a function of relative intensity of laser spots, denoted by $S_{\rm spot} : S_{\rm wall}$. (b) Flux symmetry as a function of laser injection angle $\theta_{\rm L}$. $\Delta\theta$ is the distance of deviation from the spot position of $\theta_{\rm L} = 55°$. Red line and black line represent C_{40} and $\varepsilon_{\rm rms}$, respectively.

In the design of the hohlraum, the LEH size is a very important parameter. On one hand, a sufficiently large LEH is needed to ensure the normal injection of the laser. On the other hand, a bigger LEH will cause more leakage of laser energy and lower radiation temperature in the hohlraum. With the plasma temperature rising and the plasma expanding, shrinking of LEHs occurs, which may affect not only the laser injection, but also the flux symmetry on the capsule. As shown in Fig. 3(a), with the shrinking of LEHs, they become smaller in the view field of the capsule. Therefore, the negative contribution of LEHs is reduced, and the asymmetry mode C_{40} changes from negative to positive. The total asymmetry index $\varepsilon_{\rm rms}$ reaches its minimum when $R_{\rm LEH} \approx 1.0$ mm (C_{40} approaches zero).

In the six-cylinder-port hohlraum, the relative independence of each column is very beneficial to the symmetry control, and tuning column length of the hohlraum is an important method for changing the symmetry on the capsule. As shown in Fig. 3(b), as the length of each column $L_{\rm H}$ increases, the solid angle of LEHs to the capsule decreases, C_{40} increases gradually, and the $\varepsilon_{\rm rms}$ first becomes smaller and then becomes larger. When $L_{\rm H} \approx 4.9$ mm, $\varepsilon_{\rm rms}$ is close to the minimum and the symmetry on the capsule is optimal. $L_{\rm H} = 4.852$ mm is

close to the optimal column length.

With the injection of the laser, the internal temperature of the hohlraum gradually increases, the wall material with high Z expands, the laser energy deposit area and radiation shining surface move inward (schematic shown in Fig. 4(a)).

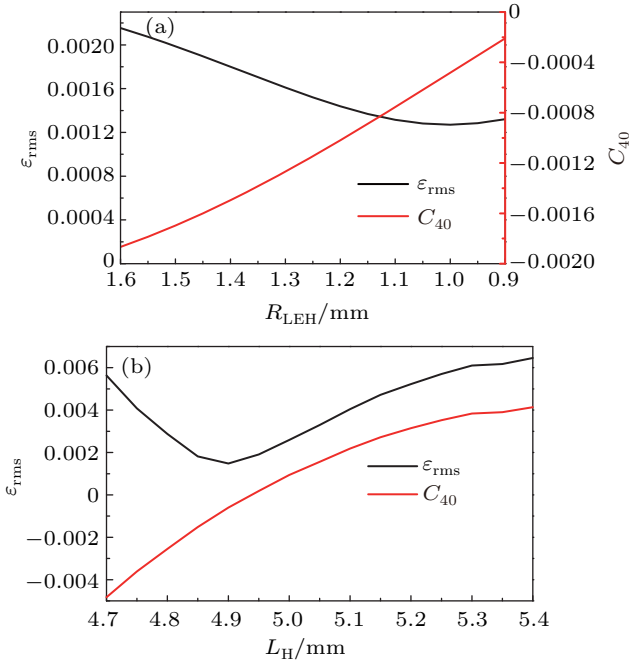


Fig. 3. (a) Flux symmetry as a function of radius of LEH $R_{\rm LEH}$. (b) Flux symmetry as a function of column length $L_{\rm H}$. Red line and black line represent C_{40} and $\varepsilon_{\rm rms}$, respectively.

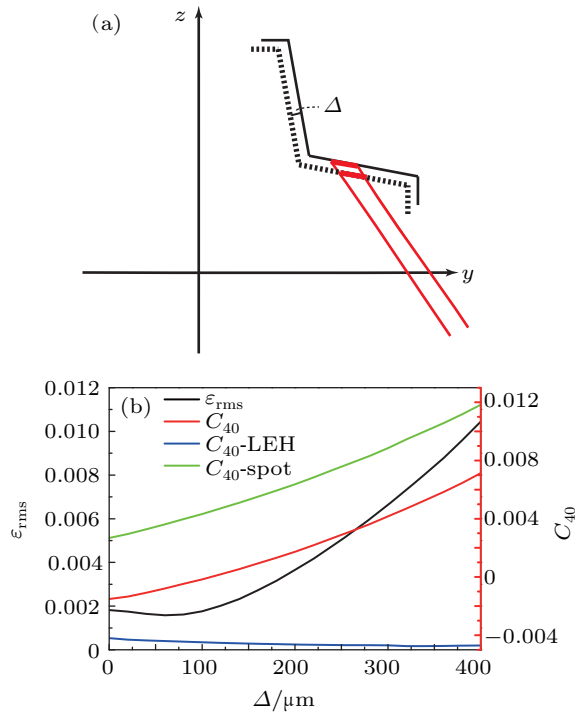


Fig. 4. Movement of laser spots affects the symmetry on capsule. (a) Schematic diagram of spot movement. (b) Flux symmetry as a function of Δ, which is the distance of movement of the hohlraum wall from the initial position. Green, blue, red, and black lines represent C_{40} contribution from spots, C_{40} contribution from LEHs, total C_{40}, and $\varepsilon_{\rm rms}$, respectively.

Figure 4(b) depicts the symmetry varying with Δ, which is the distance of movement of the hohlraum wall from the initial position. In the view field of the capsule, the inward movement of laser spots makes them reach near the capsule, and the C_{40} contribution from the spots increases gradually. While the negative contribution from LEHs keeps unchanged, the total C_{40} changes from negative to positive. When $\Delta = 70$ μm, C_{40} is close to zero, and the symmetry on the capsule is optimal.

In the preceding simulations, we do not consider the shrinking of the capsule. In the process of capsule implosion, the capsule will be highly compressed due to radiation ablation. The changes of the capsule size cause changes in the flux symmetry. We denote R_0 as the initial radius of the capsule, and $R_0/R_{\rm C}$ represents the convergence ratio. As shown in Fig. 5, in the process of capsule implosion, the convergence

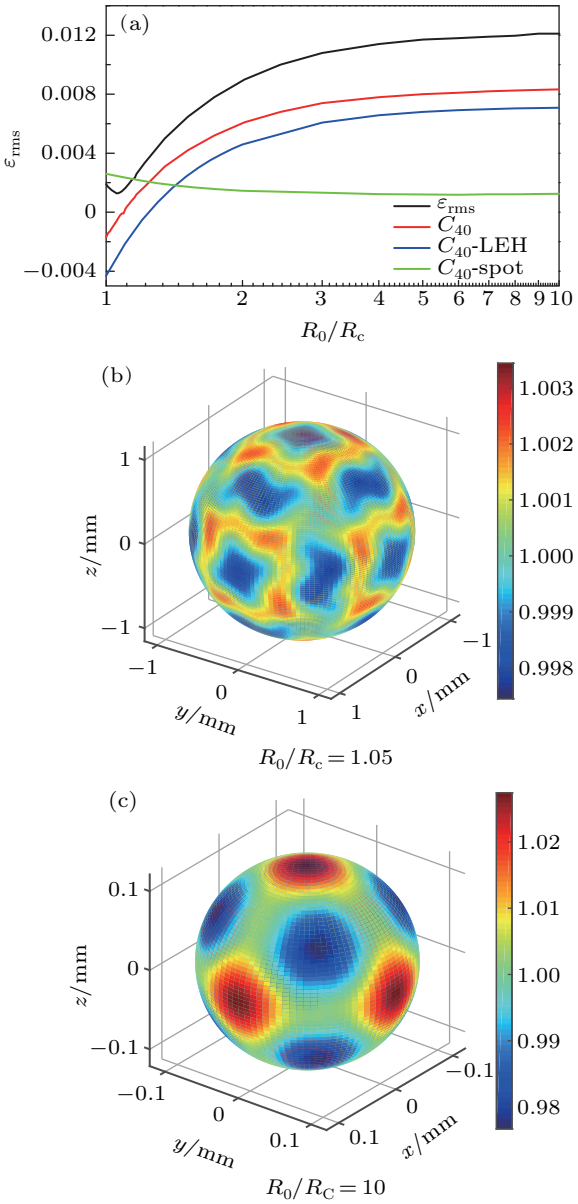


Fig. 5. Variation of symmetry with the compression of capsule. (a) Flux symmetry as a function of the convergence ratio $R_0/R_{\rm C}$. Green, blue, red, and black lines represent C_{40} contribution from spots, C_{40} contribution from LEHs, total C_{40}, and $\varepsilon_{\rm rms}$, respectively.

ratio becomes larger, and C_{40} changes from negative to positive. The C_{40} contribution from LEHs becomes zero when the distance between LEH and the capsule center is 5 times the capsule radius, and then the smooth factor changes its sign (as shown in Fig. 9.15 in Ref. [21]). So, the C_{40} contribution from LEHs changes from negative to positive. Surprisingly, with the shrinking of the capsule, the contribution from spots changes a little. When $R_0/R_C = 1.1$, $C_{40} \approx 0$, ε_{rms} is minimum, and the symmetry is optimal. In Figs. 5(b) and 5(c), at the beginning of capsule implosion, the six areas of capsule corresponding to the LEHs are dark (blue areas), and after $C_{40} > 0$, they become bright (red areas). When $R_0/R_C > 10$, ε_{rms} changes slightly, the bright and dark areas clearly separate, and the flux symmetry becomes worse.

4. Design optimization

In the design of hohlraum, the time evolution of flux asymmetry must be considered. Because the capsule can endure slightly higher asymmetry in the pre-pulse stage, but capsule is very sensitive to the asymmetry in the main-pulse stage, the hohlraum design should be optimized to endure good flux symmetry during main-pulse stage.

From the above results, we find that the asymmetry on the capsule is derived from the joint contribution of the laser spots and LEHs, and C_{40} mode is the main residual asymmetry. To control the asymmetry on the capsule in the six-cylinder-port hohlraum, we should mainly regulate the C_{40} mode. The simulation data above provide a basis for regulating the symmetry of main-pulse stage. A simple and effective method is to use the column length L_H to control the symmetry, while the other parameters are fixed, such as intensity of laser spots and other hohlraum size. The shrinking of capsule, movement of hohlraum wall, and compressing of capsule are included. It should be noticed that with the time evolution, all of them have the tendency to make C_{40} from negative to positive.

In a radiation hydrodynamic simulation of a six-cylinder-port hohlraum with geometric parameters as shown in Fig. 1(b), the movement of hohlraum wall (Δ), shrinking of LEHs (Δ_R_{LEH}), and laser power (P_L) change as a function of time, as shown in Fig. 6(a). In this simulation, foam wall material and CH liner have been used to restrain the movement of the hohlraum wall and shrinking of LEHs. When $t = 19 - 22$ ns, the laser is in the main-pulse stage, and the movement of the hohlraum wall and shrinking of LEHs are obvious. In the laser main-pulse stage, $\Delta > 70$ μm, and to have high symmetry in this stage, more negative initial C_{40} is needed. As shown in Fig. 3(b), a smaller L_H makes the initial C_{40} more negative. The flux symmetry on the capsule with different L_H values changes as a function of time, as shown in Fig. 6(b). In the hohlraum with $L_H = 4.852$ mm, ε_{rms} is optimal at $t = 10$ ns, and ε_{rms} becomes larger in the laser main-pulse stage. Smaller initial L_H makes ε_{rms} be optimal subsequently. In the $t = 19$–22 ns stage, the hohlraum with $L_H = 4.81$ mm has the best symmetry. The 3D view factor model is a highly approximate model, thus our quantitative optimization is uncertain when considering all complex physical processes in the hohlraum. In general, the six-cylinder-port hohlraum is a well-adjustable design.

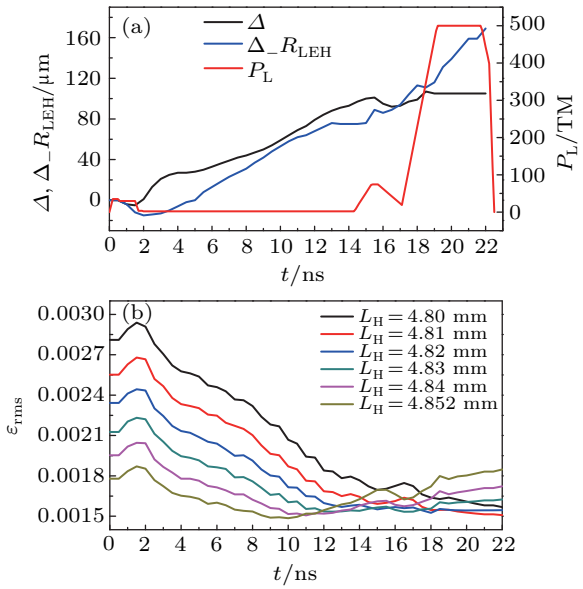


Fig. 6. (a) Movement of hohlraum wall Δ, shrinking of LEHs Δ_R_{LEH}, and laser power P_L change as a function of time. (b) Evolution of symmetry in hohlraum with different L_H values.

5. Conclusion

In indirect-drive ICF, the x-ray radiation symmetry on the capsule is an important issue for compression and ignition. The six-cylinder-port hohlraum is a new design with advantages of cylindrical geometry and laser beams arrangement with 6 LEHs, and it is predicted to have good symmetry. In this study, the factors that affect the drive symmetry of the capsule in the six-cylinder-port hohlraum, such as intensity of laser spots and laser incident angle, geometric parameters of the hohlraum, movement of hohlraum wall, and capsule compression, have been investigated.

When the C_{40} mode asymmetry approaches zero, the drive symmetry on the capsule is optimal. The changes of physical state in the hohlraum, such as movement of hohlraum wall and shrinking of LEHs, always change C_{40} from negative to positive. Changing the initial C_{40} can adjust the time at which the capsule attains the optimal symmetry. The column length L_H has been used to control the initial C_{40}. A suitable value of L_H can render the capsule better symmetry in the main-pulse stage.

In this study, the radiation on the capsule has been simulated using the 3D view factor model, which is a highly approximate model. In a future study, the symmetry obtained using the radiation hydrodynamics code will be discussed.

References

[1] Lindl J D, Amendt P, Berger R L, Glendinning S G, Glenzer S H, Haan S W, Kauffman R L, Landen O L and Suter L J 2004 *Phys. Plasmas* **2** 3933

[2] Moody J D, Callahan D A, Hinkel D E, *et al.* 2014 *Phys. Plasmas* **21** 056317

[3] Lan K, Liu J, Lai D X, Zheng W D and He X T 2014 *Phys. Plasmas* **21** 010704

[4] Lan K, He X T, Liu J, Zheng W D and Lai D X 2014 *Phys. Plasmas* **21** 052704

[5] Lan K and Zheng W D 2014 *Phys. Plasmas* **21** 090704

[6] Li X, Wu C S, Dai Z S, Zheng W D, Gu J F, Gu P J, Zou S Y, Liu J and Zhu S P 2016 *Chin. Phys. B* **25** 085202

[7] Li X, Wu C S, Dai Z S, Zheng W D, Zhao Y Q, Zhang H S, Gu J F, Ge F G, Gu P J and Zou S Y 2016 arXiv:1608.02167 [plasm-ph]

[8] Lindl J D 1995 *Phys. Plasmas* **2** 3933

[9] Lindl J D, Amendt P, Berger R L, Glendinning S G, Glenzer S H, Haan S W, Kauffman R L, Landen O L and Suter L J 2004 *Phys. Plasmas* **11** 339

[10] Hauer A A, Suter L, Delamater N, *et al.* 1995 *Phys. Plasmas* **2** 2488

[11] Duan H, Wu C S, Pei W B and Zou S Y 2015 *Phys. Plasmas* **22** 092704

[12] Huo W Y, Liu J, Zhao Y Q, Zheng W D and Lan K 2014 *Phys. Plasmas* **21** 114503

[13] Duan H, Wu C S, Pei W B and Zou S Y 2016 *Phys. Plasmas* **23** 052703

[14] Haan S W, Lindl J D, Callanhan D A, *et al.* 2011 *Phys. Plasmas* **18** 051001

[15] Michel P, Divol L, Williams E A, Weber S, Thomas C A, Callahan D A, Haan S W, Salmonson J D, Dixit S, Hinkel D E, Edwards M J, MacGowan B J, Lindl J D, Glenzer S H and Suter L J 2009 *Phys. Rev. Lett.* **102** 025004

[16] Glenzer S H, MacGowan B J, Michel P, *et al.* 2010 *Science* **327** 1228

[17] Michel P, Divol L, Town R P J, *et al.* 2011 *Phys. Rev. E* **83** 046409

[18] Moody J D, Robey H F, Celliers P M, Munro D H, Barker D A, Baker K L, Döppner T, Hash N L, Hopkins L B and Lafortune K 2014 *Phys. Plasmas* **21** 092702

[19] Kuang L Y, Li H, Jing L F, Lin Z W, Zhang L, Li L L, Ding Y K, Jiang S E, Liu J and Zheng J 2016 *Scientific Reports* **6** 34636

[20] Cohen D H, Landen O L and MacFarlane J J 2005 *Phys. Plasmas* **12** 122703

[21] Atzeni S and Meyer-ter-Vehn J 2004 *The Physics of Inertial Fusion* (Oxford: Oxford Science Press)